Evidence of In-Plane Superstructure Formation in Phase-Separated and Staged Single Crystal $La_2CuO_{4+\delta}$

X. Xiong,[1] P. Wochner,[2] S. C. Moss,[1] Y. Cao,[1] K. Koga,[3] and M. Fujita[4]
[1]*Physics Department and Texas Center for Superconductivity, University of Houston, Houston, Texas 77204-5506*
[2]*Physics Department, Brookhaven National Laboratory, Upton, New York 11973*
[3]*National Institute for Advanced Interdisciplinary Research, Tsukuba 305, Japan*
[4]*Institute of Applied Physics, University of Tsukuba, Tsukuba 305, Japan*
(Received 25 September 1995)

In single crystal $La_2CuO_{4+\delta}$, $\delta \sim 0.015$, *c*-axis interstitial oxygen ordering (staging) in the oxygen-rich phase of the phase-separated sample was observed through satellite peaks in the neutron scattering at $(0, 1, 4 \pm \sim 0.16)$ which first appear at 250 K. A superconducting $T_c \simeq 31$ K was achieved by prolonged annealing at 200 K of a staged crystal whose T_c was subsequently enhanced by $\sim$1.5 K during a 7 h cooling from 215 to 190 K. This annealing below 215 K initiates a splitting of the staging satellites along the $\mathbf{a}^*$ direction which signifies a one-dimensional modulation of the in-plane order.

PACS numbers: 74.72.Dn, 61.12.–q, 74.62.Bf

Oxygen-intercalated $La_2CuO_{4+\delta}$ is among the simplest of the family of the new superconducting Cu oxides with a superconducting T_c as high as 34 K for $0.01 \leq \delta \leq 0.05$; its structure and phase diagram have therefore attracted considerable attention [1]. Composition, pressure, and thermal history-dependent superconductivity have been observed in this material [2,5], which indicates that subtle structure modifications cause substantial changes in the superconducting properties. Although considerable progress has been made in understanding these effects, the detailed structures have, until recently, not been well determined, although phase separation into oxygen-rich and oxygen-poor regions has been observed [6–9]. Wells *et al.* [9] have, in addition, shown in single crystal neutron scattering studies of $La_2CuO_{4+\delta}$ that the oxygen-rich phases undergo, on cooling, a layering of the intercalated oxygen with attendant phase shifts of the octahedral tilts in the intervening layers as also occurs in the well-documented $La_2NiO_{4+\delta}$ studies of Tranquada *et al.* [10]. The layering is reminiscent of the staging seen in graphite intercalation compounds and may well require similar consideration of Daumas-Herold domain formation [11] in which each plane has an equal intercalant concentration which is staged. As a local probe, NMR measurements provide evidence for localized holes in the CuO_2 planes of O-doped lanthanum cuprate, and it has been shown that the anomalous copper site in the CuO_2 plane neighbors the interstitial oxygens [12]. The diffusion of single hole clusters which are space limited at $150 \leq T \leq 170$ K and space unrestricted above 180 K has also been suggested in $La_2CuO_{4+\delta}$ [13].

Adiabatic calorimetry [5] has revealed three structural phase transitions in a $La_2CuO_{4.011}$ single crystal at 287, 265, and 222 K, respectively, with different superconductivity transition temperatures for the two low temperature phases and it shall partly be our purpose here to identify structurally these transitions.

In this Letter, we report novel neutron diffraction and preliminary magnetic susceptibility results on a high quality single crystal of $La_2CuO_{4+\delta}$ with $\delta \sim 0.015$. We supply evidence for a reversible temperature-induced in-plane superstructure formation which modulates the layered-intercalated O-rich phase into which our crystal has already phase separated (as in [9]). The single crystal of $La_2CuO_{4+\delta}$ was grown by Koga *et al.* and the method was described in [8]. An as-grown crystal rod (4 mm $\times$ 10 mm) was used for the neutron experiment. Mosaic spreads along *b* and *c* directions are $5'$ (*b* axis) and $2'$ (*c* axis) as determined in [8]. The *exact* concentration of excess oxygen is not so crucial to this Letter; however, we estimate it at $\sim$0.015 by comparing our lattice parameters and the intensity ratio of the two phases that form on phase separation [for example, from the (006) splitting] with previous powder results [14].

The neutron scattering experiments were performed on the triple axis spectrometer H9 at the cold-neutron source of the High Flux Beam Reactor (HFBR) at Brookhaven National Laboratory. The double monochromator and analyzer crystals were both pyrolytic graphite set for the (002) reflection and a Be filter was employed to remove higher harmonics. Collimations were typically $60'$-$40'$-$60'$-$80'$-$80'$. The temperature was controlled using both a Displex closed-cycle He refrigerator or a liquid He cryostat for faster cooling. Part of the data was measured with an incident energy of 5 meV, while another data set used 5.1 meV to avoid multiple scattering. The crystal was oriented with b^* and c^* in the scattering plane which allows both the $(0k\ell)$ and $(h0\ell)$ zones to be measured because of twinning.

The onset temperature of phase separation (T_{PS}) into oxygen-poor ($\delta \sim 0$) and oxygen-rich ($\delta \sim 0.05$) phases and the Néel temperature (T_N) of the oxygen-poor phase ($Bmab$) were determined to be 270 and 260 K, respectively, in this single crystal. From 270 to 250 K, each

fundamental peak splits into two corresponding to the two separated phases, which can be described by space groups *Bmab* ($\delta \sim 0.0$) and *Fmmm* (disordered O, $\delta \sim 0.05$) because of the absence of splitting on mixed parity peaks [6]. In addition, a clear superstructure feature in the oxygen-rich phase appears below 250 K as observed earlier by Wells *et al.* [9].

Typical ℓ scans of the (014) reflection at 240 and 224 K after slow coolings are shown in Fig. 1. The central peak (reduced in intensity by $1/60$ in this figure) is the (014) reflection of the *Bmab* phase while both left and right peaks are first-order staging satellites of the oxygen-rich phase. The two satellites are not centered on the *Bmab* peak because of the difference in c lattice parameters for these two phases. The intensity of these staging satellite peaks arises from the tilt pattern of the Cu-O octahedra rather than from the interstitial oxygens themselves [9].

The positions of the staging satellites are controlled by the spacing between interstitial oxygen layers or antiphase domain boundary spacing [10]. At 250 K, when the satellites first appear on cooling, their positions correspond to stage 7. This means that between every 7 layers of Cu-O octahedra (3.5 unit cells) a partially occupied layer of oxygen interstitials is inserted, which leads to a tilt pattern with periodicity $7c$. The position of the satellites is temperature dependent, shown in the inset of Fig. 1, and saturates below 213 K corresponding to a staging of 6.5. Time dependence, especially at lower temperature, is observed as well. On heating, the satellites disappeared around 260 K and therefore show $\sim$10 K hysteresis in this ordering.

In fitting the staging peaks in Fig. 1 a model of random mixing of staging phases has been successfully employed to interpret these phases as in $La_2NiO_{4+\delta}$ [10] and $La_2CuO_{4+\delta}$ [9]. The first-order satellites observed here can thus be quantitatively understood by using a random mixture of stage 6 and stage 7. Originally, to explain staging changes without c-axis diffusion in the graphite intercalation compounds, the Daumas-Herold domain formation model was introduced [11]. For all of these Daumas-Herold domains the c-axis periodicity is the same, and the intercalant layers of adjacent domains are separated on average in the c direction by the same number of host layers. Intralayer diffusion with a concomitant change of domain sizes and distribution thus enables staging changes. The driving force is the elastic energy associated with the lattice distortion by the intercalant atoms which increases with higher order staging [11]. A similar mechanism is also expected to enable staging changes in all oxygen-intercalated $La_2MO_{4+\delta}$ (M = Cu, Ni, Mn) compounds. The temperature dependence of the integrated intensity of an ℓ scan through $(0, 1, 4 + \Delta)$ ($\Delta \approx 0.150-0.153$) is shown in Fig. 2 together with the annealing schedule which we followed in this very slow cooling. Open symbols represent data points obtained on heating.

Clearly, the temperature dependence of the satellite intensity is very different from the one Wells *et al.* [9] observed for non-phase-separating samples which show a continuous increase and saturation of the intensity below $\sim$50 K as well as constant staging. In our study, below 213 K the intensity drops coinciding with a lock-in of the staging. To understand this drop of intensity at 213 K we performed k scans, radial scans, rocking scans, and χ scans (the last essentially normal to the $0k\ell$ plane, along h) of the $(0, 1, 4 + \Delta)$ ($\Delta = 0.153$) satellite. The full width at half maximum (FWHM) of all scans in the $0k\ell$ plane are basically temperature independent. Figure 3 shows the fitted results of the χ scans, cooling from 213 down to 187 K over a 20 h period. Fits at 213, 203,

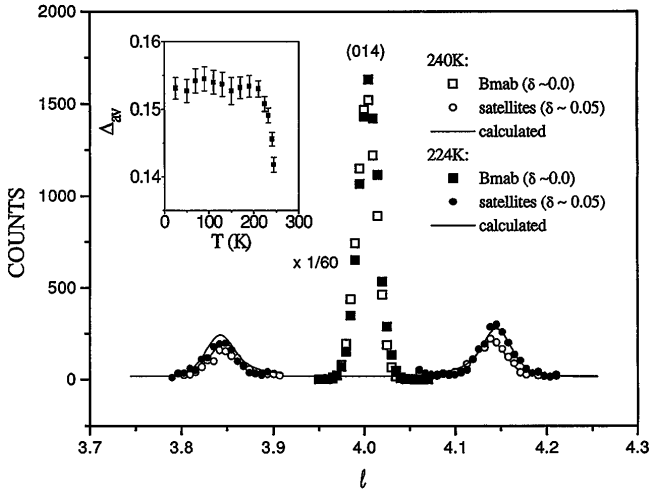

FIG. 1. Appearance of the first-order satellite pair (counting 120 sec per scan step) in a slow cooling to 240 and 224 K in the oxygen-rich phase ($\delta \sim 0.05$); the middle peak (counting 2 sec per scan step) is the reflection (014) of the *Bmab* phase ($\delta \sim 0.0$). The line is the calculated intensity using a simple staging model for each temperature (see text). The inset shows the temperature dependence of the satellite peak position.

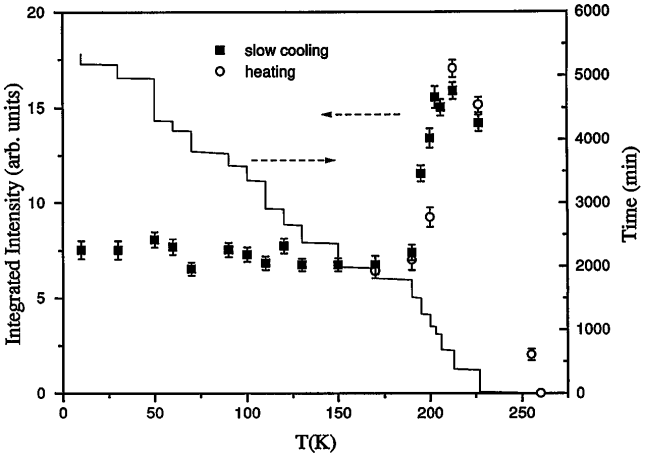

FIG. 2. Integrated intensity of the satellite peaks at $(0, 1, 4 + \Delta)$ vs temperature in slow cooling from 280 to 10 K. Full squares: cooling; open circles: subsequent heating.

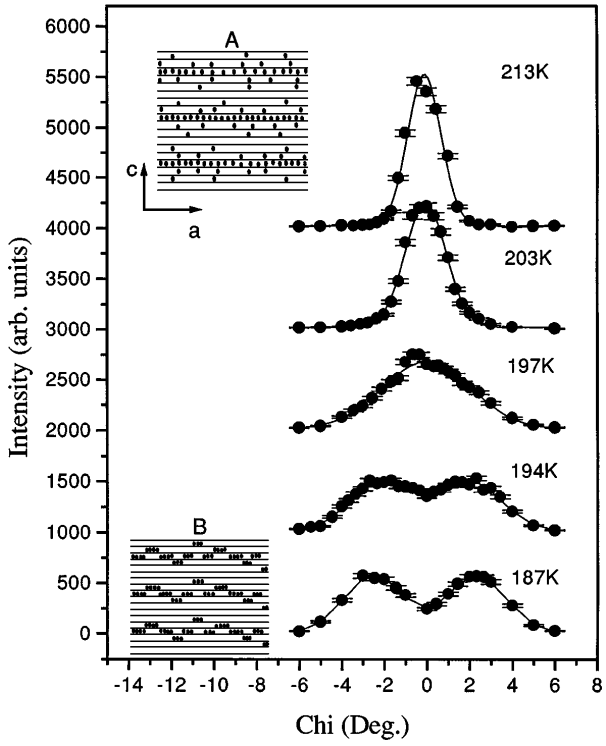

FIG. 3. χ scans of the staging satellite at $(0, 1, 4.153)$ as a function of cooling with each displaced vertically by 1000 units. These scans are essentially along h at fixed k, ℓ and each was taken after a period of $\sim$2 h at each temperature; the fits are by single Gaussian (213, 203, and 197 K) and by two Gaussians (194 and 187 K); see Table I for fit values. Insets are presented for 213 K (model A) and 187 K (model B) representing schematically the oxygen arrangements appropriate to these temperatures (see text and Ref. [15]). The lines are CuO layers and the circles are interstitial oxygens. Both insets have the same a and c axes.

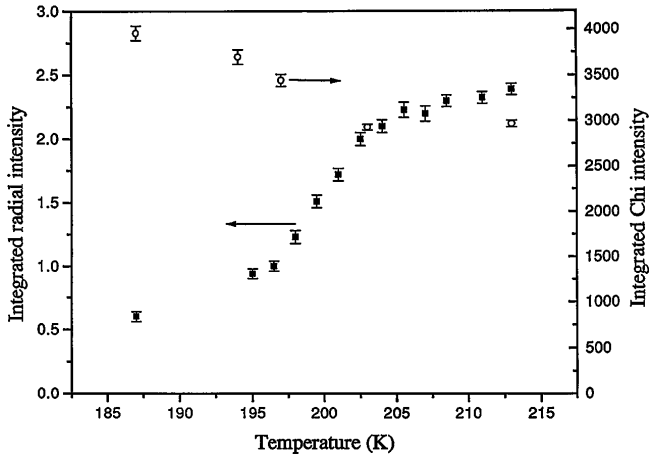

FIG. 4. Integrated intensities as a function of temperature for the $(0, 1, 4.153)$ staging satellite (left scale—radial intensity) and over the entire χ scan covering both $(0, 1, 4.153)$ and its h-split components (right scale—chi intensity).

and 197 K can be made using one (albeit broadened) Gaussian while at 194 and 187 K two peaks are required whose positions and widths change with temperature. The FWHM at 225 K ($\sim$2.0°) is resolution limited.

We include in Fig. 3 schematic representations of the oxygen distribution appropriate to the single staging peak ($h = 0$) at 213 K (model A) and to the split peaks along $h(a^*)$ at 187 K (model B). These distributions pertain to a *single* Daumas-Herold domain, with a given intercalant plane, in which the oxygen is weakly spread over adjacent planes at 213 K and is sharply modulated at 187 K giving rise essentially to "antiphase domain" satellites along h. For a detailed presentation of the quantitative fits to these, and more recent data, we refer the reader to Ref. [15].

The integrated intensities of radial scans through $(0, 1, 4.153)$, which show only a single peak, are plotted versus temperature in Fig. 4 together with the integrated χ intensity over all the peaks in Fig. 3. We interpret the drop of intensity in the radial scan as the occurrence of a phase transition expressing the in-plane ordering illustrated in the insets in Fig. 3. The integrated χ intensity shows more intensity in the satellites along $h(\mathbf{a}^*)$ than is contained originally at the $\Delta = 0.153$ position. This may well be due to the collection of a substantial diffuse scattering into these in-plane peaks on in-plane ordering as well as to an elastic relaxation on ordering which restores the intensity to these peaks in a manner analogous to a diminished static Debye-Waller factor.

Table I presents the results of our fits to the χ scans at the five temperatures of Fig. 3. The widths and intensities are significant and at 194 and 187 K the clear $\chi(h)$ splitting reveals the development of the periodic in-plane modulation of, respectively, 76 and 63 Å. This static domain formation is perforce one dimensional (i.e., stripelike) as it occurs only along **a**. Part of the width of the χ scans is due to orthorhombic twinning. Therefore, each of the two peaks in χ is composed of two twin-related

Table I. Results of the fits to χ about $(0, 1, 4.153)$.

T (K)	χ position expressed in h units (r.l.u.)	FWHM in chi scan expressed in h units (r.l.u.)	Integrated intensity in chi scan (arb. units)
213	−0.0034(4)	0.0634(7)	2966(38)
203	−0.0017(4)	0.077(1)	2930(33)
197	0.000(1)	0.165(3)	3444(67)
194			
Peak 1	−0.073(2)	0.117(4)	1827(66)
Peak 2	0.068(2)	0.122(5)	1870(71)
187			
Peak 1	−0.085(2)	0.110(4)	1980(60)
Peak 2	0.079(2)	0.111(3)	1977(55)

partners. On heating, the disappearance of the χ splitting shows a $\sim$5 K hysteresis indicative of pronounced nucleation and growth kinetics and a first-order phase transition. Quenching experiments, where we cool the sample in 80 sec from 300 to 190 K, and which suppress the phase separation, followed by controlled annealing show that the diffusion of oxygen is responsible for the growth kinetics of the satellite peaks.

None of the reflections of the oxygen-poor phase and none of the fundamental peaks show splitting in χ. An extensive search in all high symmetry directions of the $b^*(a^*)$-c^* plane found no satellite peaks other than the ones due to c-axis staging. Ryder *et al.* [1] observed in electron microscope dark field images the development of a pronounced fringe pattern in the a^* direction (*Bmab* notation) on cooling to 100 K with a periodicity decreasing from 1500 down to $\sim$300 Å. Their interpretation of a periodic ordering of oxygen-poor and oxygen-rich regions seems to disagree with the lack of any additional in-plane superstructures of the oxygen-poor phase. For the present, additional neutron experiments are confirming the behavior reported here and our modeling, as noted above, indicates that our interpretation is essentially correct [15].

The magnetic measurements based on our neutron experience indeed show a small, but reproducible, superstructure-enhanced superconductivity. Figure 5 indicates an enhancement of T_c of $\sim$1.5 K. This change comes from a comparison of the annealing of a small crystal (cut from our neutron sample) at $\sim$200 K for 30 min after cooling it slowly to 227 K (seq. a) with cooling it from 215 to 190 K over 7 h (seq. b) as discussed above. The measurements were done in the zero field cooling (ZFC) mode with the b axis aligned with the field

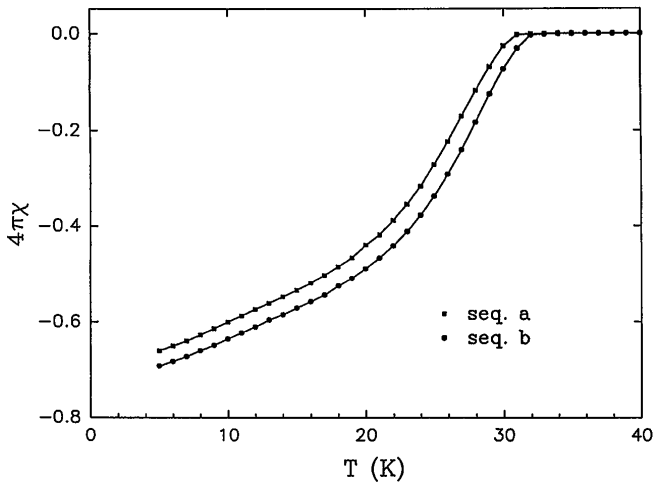

FIG. 5. ZFC magnetic measurements for seq. a and seq. b. The applied magnetic field is 5 G and is parallel to the b axis. Seq. b represents a long anneal from 210 to 190 K while seq. a is for an anneal at 200 K for 30 min after cooling slowly to 227 K followed by a quench.

and show a real effect of the in-plane domain ordering on T_c. Annealing effects on T_c have been reported in the literature [4,5,13]. Our finding presents direct evidence for structural changes to be involved in this enhancement of T_c. In other high T_c materials, e.g., $Ba_2Sr_2CaCu_2O_8$, annealing procedures have also been shown to improve the superconducting T_c [16].

Regarding the recent calorimetric observations [5] of three structural phase transitions in $La_2CuO_{4.011}$, we conclude that the one at 265 K corresponds to the c-axis staging transition (260 K on heating in our case) and the first-order transition at 222 K to the new in-plane superstructure which disappears at $\sim$218 K on heating. Kyomen *et al.* [5] also find a T_c of 33 K for the phase above 222 K with an increase to 40 K for the phase below.

We expect that the new in-plane superstructure reported here may also appear in non-phase-separating $La_2CuO_{4+\delta}$ samples with higher oxygen concentrations and in $La_2NiO_{4+\delta}$ compounds. A large periodicity and poor χ resolution might have thus far prevented their observation. In a phase-separating sample of $La_2NiO_{4.06}$ this effect may have already been observed indirectly [10].

We acknowledge helpful discussions with J. M. Tranquada, J. D. Axe, P. C. Chow, P. H. Hor, and H. H. Feng on various aspects of this work, which was supported at Houston by the Texas Center for Superconductivity (TCSUH) and the NSF by Grant No. DMR-9208420 and at BNL by the Division of Materials Research, U.S. DOE Contract No. DE-AC-02-76CH00016.

[1] See, for example, J. E. Schirber *et al.*, Physica (Amsterdam) **152C**, 121 (1988); J. Ryder *et al.*, Physica (Amsterdam) **173C**, 9 (1991); J.-C. Grenier *et al.*, Physica (Amsterdam) **202C**, 209 (1992); P. G. Radaelli *et al.*, Phys. Rev. B **48**, 499 (1993); P. C. Hammel *et al.*, Phys. Rev. Lett. **71**, 440 (1993).
[2] See, for example, H. H. Feng *et al.*, Phys. Rev. B **51**, 16 499 (1995).
[3] M. Itoh *et al.*, Phys. Rev. B **51**, 1286 (1995).
[4] E. T. Ahrens *et al.*, Physica (Amsterdam) **202C**, 317 (1993).
[5] T. Kyomen *et al.*, Phys. Rev. B **51**, 3181 (1995).
[6] J. D. Jorgensen *et al.*, Phys. Rev. B **38**, 11 337 (1988).
[7] C. Chaillout *et al.*, Physica (Amsterdam) **170C**, 87 (1990).
[8] K. Koga *et al.*, J. Phys. Soc. Jpn. **64**, 3365 (1995).
[9] B. Wells *et al.* (to be published).
[10] J. M. Tranquada *et al.*, Phys. Rev. B **50**, 6340 (1994).
[11] G. Kirczenow, in *Graphite Intercalation Compounds I*, edited by H. Zabel and S. A. Solin (Springer-Verlag, New York, 1990), p. 59.
[12] P. C. Hammel *et al.* (to be published).
[13] R. K. Kremer *et al.*, Z. Phys. B **91**, 169 (1993).
[14] P. G. Radaelli *et al.*, Phys. Rev. B. **49**, 6239 (1994).
[15] P. Wochner *et al.* (to be published).
[16] L. Vasiliu-Doloc (private communication).